ONCOhabitats glioma segmentation model

Javier Juan-Albarracín[1], Elies Fuster-Garcia[1,2] [0000-0002-0716-8960], María del Mar Álvarez-Torres[1], Eduard Chelebian[1], and Juan M. García-Gómez[1]

[1] Instituto Universitario de Tecnologías de la Información y Comunicaciones, Universitat Politècnica de València, València, Spain
{jajuaal1, juanmig}@itaca.upv.es
maaltor4@upv.es
edchekoc@etsii.upv.es
[2] Department of Diagnostic Physics, Oslo University Hospital, Oslo, Norway
elfusgar@upv.es

Abstract. ONCOhabitats is an open online service that provides a fully automatic analysis of tumor vascular heterogeneity in gliomas based on multiparametric MRI. Having a model capable of accurately segment pathological tissues is critical to generate a robust analysis of vascular heterogeneity. In this study we present the segmentation model embedded in ONCOhabitats and its performance obtained on the BRATS 2019 dataset. The model implements an residual-Inception U-Net convolutional neural network, incorporating several pre- and post-processing stages. A relabeling strategy has been applied to improve the segmentation of the necrosis of high-grade gliomas and the non-enhancing tumor of low-grade gliomas. The model was trained using 335 cases from the BraTS 2019 challenge training dataset and evaluated with 125 cases from the validation set and 166 cases from the test set. The results on the validation dataset in terms of the mean/median Dice coefficient are 0.73/0.85 in the enhancing tumor region, 0.90/0.92 in the whole tumor, and 0.78/0.89 in the tumor core. The Dice results obtained in the independent test are 0.78/0.84, 0.88/0.92 and 0.83/0.92 respectively for the same sub-compartments of the lesion.

Keywords: glioma, convolutional neural network, segmentation.

1 Introduction

Gliomas are one of the most common central nervous system (CNS) tumors. Gliomas comprise a very diverse group of CNS tumors that vary histologically from low grade (LGGs; grade II) to high grade (HGGs; Grades III, IV)[1]. Knowing the extent and the heterogeneity of the lesion is crucial to make a correct diagnosis, plan radiotherapy treatment, analyze the response to treatment, and monitor the progression of the disease. Manual segmentation and volumetric studies of the different glioma tissues involves an arduous, time-consuming and often unaffordable task for humans, that is not often performed in clinical practice but only in some clinical studies.

In recent years, and with the emergence of new deep learning technologies, a substantial effort has been made to generate models capable of automatically delineate glioma pathologic tissues with high accurate confidence. An example of the effort invested in this task is the creation of the multimodal BRain Tumour Segmentation (BRATS) challenge. Since 2012 and until now, numerous researchers have focused their efforts on generating more accurate brain tumor segmentation models, reaching computational models with a performance close to human expert labelling [2]. Nevertheless, there is still a need for more research to achieve completely reliable segmentation models that can handle the wide range of heterogeneous tumors that can arise in real clinical routine.

This work presents a segmentation model of gliomas that consists on a patch-based 3D U-net Convolutional Neural Network based on residual-Inception blocks. The preprocessing includes noise reduction, bias correction, and intensity normalization. A relabeling strategy was applied to differentiate HGG necrosis and LGG non-enhancing tumor in the training stage. Finally, a postprocessing stage was implemented to remove spurious or incoherent segmentation objects.

The proposed tumor segmentation model is included in the last version of ONCOhabitats [3] online platform (https://www.oncohabitats.upv.es), provided by the Polytechnic University of Valencia [4]. ONCOhabitats provides a fully automatic analysis of tumor vascular heterogeneity, four vascular habitats within the lesion from MRI images: the High Angiogenic Tumor (HAT), the Low Angiogenic Tumor (LAT), the Infiltrated Peripheral Edema (IPE) and the Vasogenic Peripheral Edema (VPE) [5]. ONCOhabitats includes two main services: (1) glioma tissue segmentation based on CNN; and (2) vascular heterogeneity assessment. In addition, we provide to researchers and clinicians our computational resources, including a system able to process about 300 cases per day including image preprocessing and standardization, regions of interest (ROIs) segmentation, perfusion quantification and vascular heterogeneity assessment of the lesion.

2 Materials

To train the proposed model, only the images provided in the 2019 edition of the BRATS challenge were used [2], [8], [9], [10], [11] . The training dataset includes 335 studies, each one composed by pre- and post-contrast T1-weighted MRI, as well as T2-weighted, T2-fluid attenuated inversion recovery (FLAIR) MRI. Additionally, the ground truth maps are provided, distinguishing between 3 labels: label 1, which encloses necrosis, non-enhancing tumor, cyst and hemorrhage tissues; label 2, which delineates the edema; and label 4 that represents the enhancing tumor. The validation dataset comprises 125 images while the test set is composed of 166 images, both including the same MRI sequences but without the ground truth maps. An online oracle is provided to evaluate the proposed models in a blind manner.

2.1 Preprocessing

BRATS2019 dataset preprocessing performed by the organizers includes: 1) voxel isotropic resampling to $1mm^3$, 2) intra-patient registration to the T1ce sequence and inter-patient registration to a common reference space, and 3) skull-stripping for cranium removal.

We have extended this preprocessing by including a denoising stage using the Adaptive Non-Local Means filter proposed in [12]. We employed search windows of 7x7x7 and a patch window of 3x3x3, with Rician noise model. Additionally, a bias field correction stage was performed using N4ITK software at different scale levels [13], with 150 B-splines. Finally, z-score normalization was performed for each image, only normalizing the voxels within the brain (i.e. excluding the background from the normalization).

3 Methods

We propose a patch-based 3D U-net Convolutional Neural Network based on residual-Inception blocks. The network takes as input 3D patches of 64x64x64 of three channels being the T1 contrast enhanced, the T2 and the Flair sequences. T1 sequence was discarded due to a worsening of the results when including it in the learning process. Therefore, the network works with patches of 64x64x64x3. The architecture details are described below.

3.1 Architecture

A U-net with 4 levels of depth is designed. The encoding path includes 3 *downsampling blocks* consisting of Conv 3x3x3 (stride 2x2x2) + ReLU + Batch Normalization. Likewise, the decoding path incorporates 3 analogous *upsampling blocks* consisting of: TransposeConv 3x3x3 (stride 2x2x2) + ReLU + Batch Normalization. Hence, the downsampling and upsampling operations are learnt by the network instead of using Max Pooling or repeatable Upsampling operations.

The network is composed of 4 levels with 24, 48, 96, 192 filters at each level respectively. Each level contains a Residual-Inception module to capture features at different scales. The residual-Inception block has 4 parallel paths with the following structure:

- Conv 1x1x1-NF + ReLU + Batch Normalization
- Conv 3x3x3-NF + ReLU + Batch Normalization
- Conv 3x3x3-NF + ReLU + Batch Normalization + Conv 3x3x3-NF + ReLU + Batch Normalization
- Max Pooling 3x3x3 (stride 1x1x1) + Conv 1x1x1-NF + ReLU + Batch Normalization,

where NF refers to the *Number of Filters* depending on the level of the U-net in which the Residual-Inception block is. The output of these 4 paths is then feed to a concatenation layer and the output is passed to a block of the form: *Conv 1x1x1-NF + ReLU +*

Batch Normalization, to compress the information extracted by the 4 paths. Finally, a residual connection is introduced by summing the input of the Residual-Inception block to the output. Figure 1 shows a diagram of the Residual-Inception block. Note that each *Simple block* (except the Max Pooling) includes a Convolution + ReLU + Batch Normalization layers. Additionally, long-skip connection between symmetric levels are introduced to allow a better gradient flow during training process. Figure 2 shows a diagram of the network architecture used in the study.

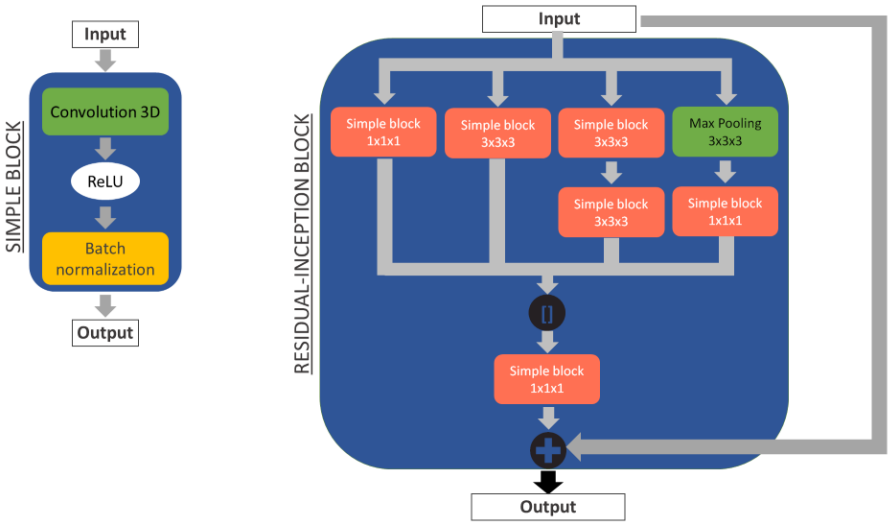

Fig. 1. Diagram of the Residual-Inception block used in our model.

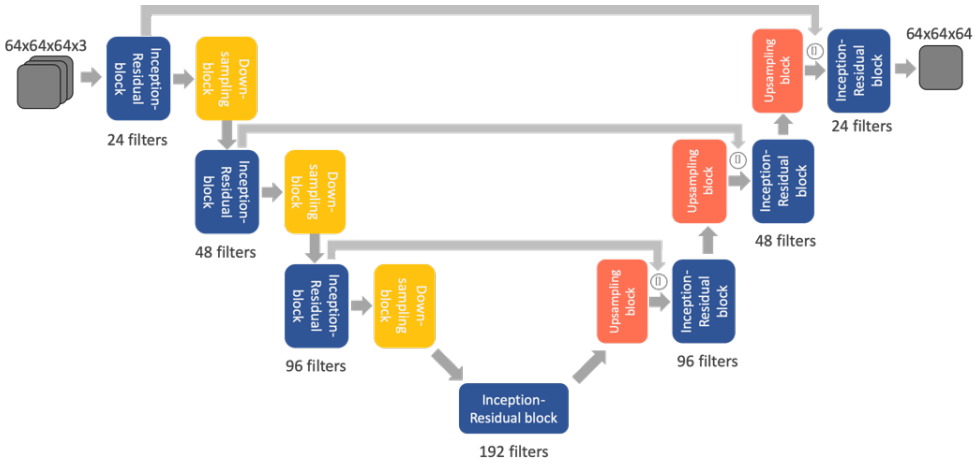

Fig. 2. Diagram of the 4-level residual network architecture. Residual-Inception blocks are used as feature extraction modules. Downsampling and upsampling operations are performed through strided conventional and transposed convolutions. Long concatenation-skip-connections are employed between symmetric levels.

3.2 Training strategy

Label 1 in the BRATS 2019 dataset encloses a set of different glioma tissues, including necrosis, non-enhancing tumor, cyst, hemorrhage, etc. Such tissues largely differ in appearance in the MRI images, so in order to simplify the learning task for the network we decided to re-label the label 1 in all the LGG cases by label 3. Such re-labelling pursues the idea of associating the label 1 mostly to the necrosis tissue, typically present in HGG; and the label 3 to the non-enhancing tumor tissue, typically predominant in LGG.

We followed a balanced training strategy by creating batches containing a uniform proportion of patches containing predominantly edema (label 2), necrosis (label 1), enhancing tumor (label 4), non-enhancing tumor (label 3) and healthy tissues (label 0). Due to memory restrictions, batches of 4 samples was employed to train the network.

We also employed a combined loss consisting on the unweighted sum of cross-entropy and dice losses. Additionally, we trained the network with label smoothing with a factor 0.1, to relax the confidence in the labels. Adam optimizer was used with a starting learning rate of 1e-3. We trained the network 35k iterations.

3.3 Postprocessing

In order to remove spurious or incoherent segmentation components, we developed a simple postprocessing stage based on Connected Components (CC) analysis. As a *rule of thumb,* we always save the biggest CC as it is the most probable that contains the correct segmentation. The remaining CCs are analyzed and saved only if they met the following criteria:

1. The CC contains a number of voxels of class 4, class 3 or class 1 greater than the 5% of the size of the CC.
2. The CC has more than 1000 voxels

Such simple post-processing mostly intends to discard erroneous CCs produced by magnetic bias field inhomogeneities in the images. Typically, these CCs are mainly labeled as class 2 (edema-like pattern), due to hyperintensities in Flair or T2 images. Thus, by the opposite, if the CC contains voxels segmented as enhancing tumor, non-enhancing tumor or necrosis, it can serve as an indicator of the confidence in the segmentation of the CC. Anyway, if the CC is big enough (more than 1000 voxels) we also assume that it is not an inhomogeneity artifact and the CC is saved for the final segmentation.

4 Results

The results obtained by ONCOhabitats glioma segmentation model on the independent validation dataset provided by BraTS 2019 challenge are summarized in Table 1. Dice, Sensitivity, Specificity and Hausdorff95 Distance metrics are reported.

Table 1. Summary of the results obtained by ONCOhabitats glioma segmentation model on the independent validation dataset for Enhancing Tumor (ET), Whole Tumor (WT) and Tumor Core (TC) regions.

	Dice			Sensitivity			Specificity			Hausdorff95		
	ET	WT	TC	ET	WT	TC	ET	WT	TC	ET	WT	TC
Mean	0.73	0.90	0.78	0.78	0.88	0.75	1.00	1.00	1.00	4.25	5.06	7.80
Std.Dev.	0.29	0.08	0.25	0.27	0.11	0.27	0.00	0.01	0.00	7.50	6.59	11.7
Median	0.85	0.92	0.89	0.87	0.91	0.87	1.00	1.00	1.00	2.24	3.16	3.39
25QT	0.73	0.89	0.73	0.77	0.85	0.64	1.00	0.99	1.00	1.41	2.24	2.00
75QT	0.90	0.94	0.94	0.95	0.95	0.94	1.00	1.00	1.00	3.32	5.10	9.26

Additionally, box plot of the distribution of the Dice, sensitivity and specificity metrics for the cases on the independent validation dataset evaluated on the Enhancing Tumor (ET), Whole Tumor (WT) and Tumor Core (TC) regions are presented in Figure 2.

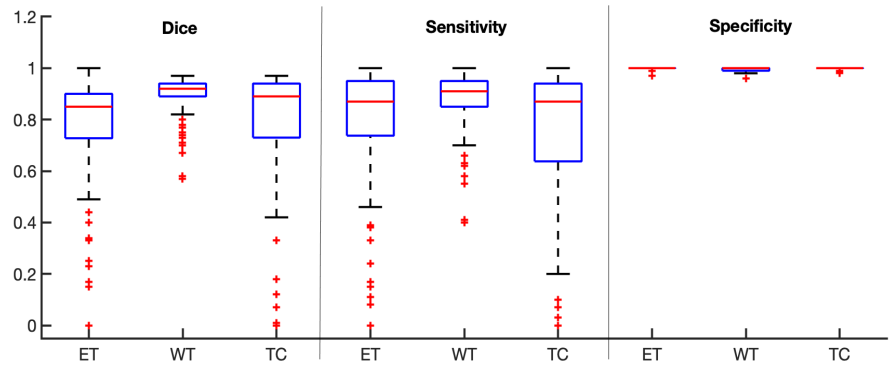

Fig. 3. Box plot showing the distribution of the Dice, sensitivity and specificity metrics for the cases on the independent validation dataset evaluated on the Enhancing Tumor (ET), Whole Tumor (WT) and Tumor Core (TC) regions.

Similarly, the results obtained by the ONCOhabitats model on the test dataset are presented in Table 2.

Table 2. Summary of the results obtained by ONCOhabitats glioma segmentation model on the test dataset for Enhancing Tumor (ET), Whole Tumor (WT) and Tumor Core (TC) regions.

	Dice		
	ET	WT	TC
Mean	0.78	0.88	0.83
Std.Dev.	0.22	0.11	0.25
Median	0.84	0.92	0.92
25QT	0.77	0.87	0.86
75QT	0.91	0.95	0.95

Figure 4 shows a comparison between the results of our model in the validation and the test set. An overall stable performance of the mean Dice is demonstrated, indicating that the model is robust against unseen samples and suggest no overfitting. Moreover, the ET and TC regions showed an improved performance in the test dataset with respect to the validation dataset. Finally, comparing our Dice results in the Whole Tumor subcompartment with the Validation Leaderboard ranking, there is a small difference of 0.01687 Dice points with respect to the 1st place team, but using a small and therefore fast network.

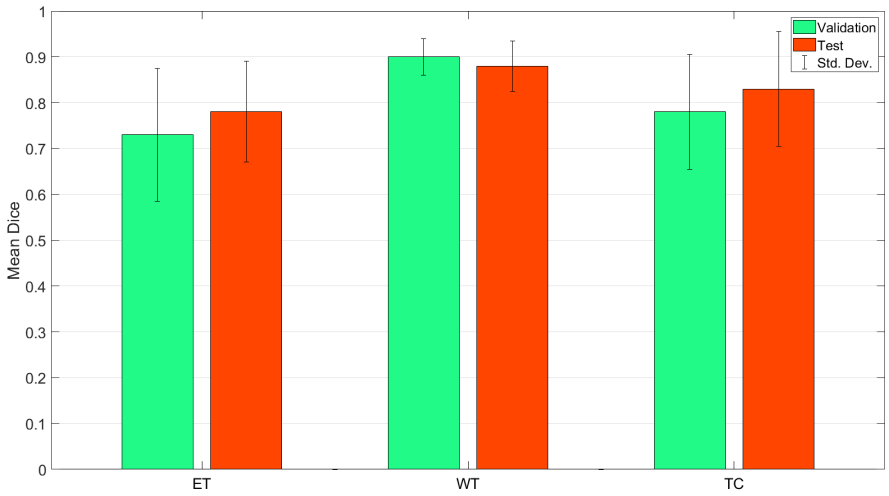

Fig. 4. Bar plot showing the mean Dice for the cases on the independent Validation and Test dataset evaluated on the Enhancing Tumor (ET), Whole Tumor (WT) and Tumor Core (TC) regions. The error bars represent the standard deviation.

Finally, Figure 5 shows the segmentation results of several cases of the test dataset.

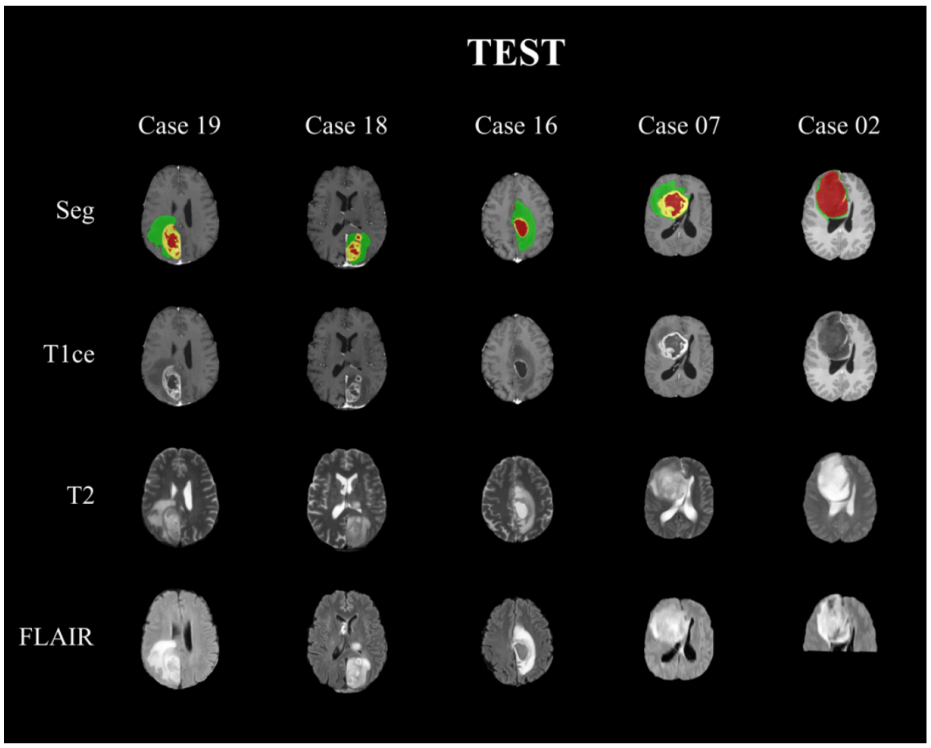

Fig. 5. Examples of glioma segmentation of 5 cases from the test set. First row shows the segmentation performed by the ONCOhabitats model over the T1ce sequence. Second, third and fourth rows show the T1ce, T2 and FLAIR sequences respectively.

5 Conclusions

In this work, we propose a glioma segmentation model based on a residual U-Net residual CNN together with an additional imaging pre- and post-processing stages to remove spurious or incoherent segmentation objects. This segmentation model has been trained using a relabeling strategy aimed to improve the segmentation of HGG necrosis and LGG non-enhancing tumor. The proposed model is included in the current version of ONCOhabitats open online service (https://www.oncohabitats.upv.es).

The results obtained show and improvement on the performance of the previous segmentation model included on ONCOhabitats reported in [3]. This allows to signifi-

cantly improve the other services provided by ONCOhabitats, such as the vascular heterogeneity assessment service, since they use as basis the glioblastoma segmentation module.

6 Acknowledgements

This work was partially supported by: MTS4up project (National Plan for Scientific and Technical Research and Innovation 2013-2016, No. DPI2016-80054-R) (JMGG); H2020-SC1-2016-CNECT Project (No. 727560) (JMGG) and H2020-SC1-BHC-2018-2020 (No. 825750) (JMGG) and CaixaImpulse program from Fundació Bancaria "La Caixa" (LCF/TR/CI16/10010016). M.A.T was supported by DPI2016-80054-R (Programa Estatal de Promoción del Talento y su Empleabilidad en I+D+i). We gratefully acknowledge the support of NVIDIA Corporation with the donation of the Titan V GPU used for this research. EFG was supported by the European Union's Horizon 2020 research and innovation programme under the Marie Skłodowska-Curie grant agreement No 844646.

References

[1] D. N. Louis *et al.*, "The 2016 World Health Organization Classification of Tumors of the Central Nervous System: a summary," *Acta Neuropathologica*, vol. 131, no. 6, pp. 803–820, Jun. 2016.

[2] B. H. Menze *et al.*, "The Multimodal Brain Tumor Image Segmentation Benchmark (BRATS)," *IEEE Trans Med Imaging*, vol. 34, no. 10, pp. 1993–2024, Oct. 2015.

[3] J. Juan-Albarracín, E. Fuster-Garcia, G. A. García-Ferrando, and J. M. García-Gómez, "ONCOhabitats: A system for glioblastoma heterogeneity assessment through MRI," *International Journal of Medical Informatics*, vol. 128, pp. 53–61, Aug. 2019.

[4] "ONCOHabitats - Glioblastoma segmentation - MRI," *ONCOHabitats*. [Online]. Available: https://www.oncohabitats.upv.es/. [Accessed: 09-Aug-2019].

[5] J. Juan-Albarracín *et al.*, "Glioblastoma: Vascular Habitats Detected at Preoperative Dynamic Susceptibility-Weighted Contrast-Enhanced Perfusion MR Imaging Predict Survival.," *Radiology*, Epub ahead of print 2018.

[6] E. Fuster-Garcia, J. Juan-Albarracín, G. A. García-Ferrando, L. Martí-Bonmatí, F. Aparici-Robles, and J. M. García-Gómez, "Improving the estimation of prognosis for glioblastoma patients by MR based hemodynamic tissue signatures," *NMR in Biomedicine*, vol. 31, no. 12, p. e4006, Dec. 2018.

[7] Álvarez-Torres, M., Juan-Albarracín, J. , Fuster-Garcia, E. *et al*. Robust association between vascular habitats and patient prognosis in glioblastoma: An international multicenter study. J Magn Reson Imaging 2019. doi:10.1002/jmri.26958

[8] S. Bakas *et al.*, "Advancing The Cancer Genome Atlas glioma MRI collections with expert segmentation labels and radiomic features," *Sci Data*, vol. 4, p. 170117, 05 2017.

[9] S. Bakas *et al.*, “Identifying the Best Machine Learning Algorithms for Brain Tumor Segmentation, Progression Assessment, and Overall Survival Prediction in the BRATS Challenge,” *arXiv:1811.02629 [cs, stat]*, Nov. 2018.

[10] S. Bakas *et al.*, “Segmentation Labels for the Pre-operative Scans of the TCGA-GBM collection.” The Cancer Imaging Archive, 2017.

[11] S. Bakas *et al.*, “Segmentation Labels for the Pre-operative Scans of the TCGA-LGG collection.” The Cancer Imaging Archive, 2017.

[12] D. L. Coupé P. ,. Manjón, J. V. ,. Robles, M. ,. Collins, “Adaptive multiresolution non-local means filter for three-dimensional magnetic resonance image denoising,” *IET Image Processing*, vol. 6, no. 5, pp. 558–568, 2012.

[13] N. J. Tustison *et al.*, “N4ITK: improved N3 bias correction,” *IEEE Trans Med Imaging*, vol. 29, no. 6, pp. 1310–1320, Jun. 2010